

The 1st International Joint Mini-Symposium on Advanced Coatings between Indiana University-Purdue University Indianapolis and Changwon National University

## Microstructure evolution and thermal durability with coating thickness in APS thermal barrier coatings

Z. Lu<sup>a</sup>, S.W Myoung<sup>a</sup>, E.H. Kim<sup>a</sup>, J.H. Lee<sup>a</sup>, Y.G. Jung<sup>a,\*</sup>

<sup>a</sup>*School of Materials Science and Engineering, Changwon National University, Changwon, Gyeongnam 641-773, Republic of Korea*

---

### Abstract

The effects of the coating thickness on the delamination or fracture behavior of thermal barrier coatings (TBCs) were investigated through the cyclic furnace thermal fatigue (CFTF) and thermal shock (TS) tests. The TBCs were prepared using a NiCrAlY bond coat and an yttria-stabilized zirconia top coat, which were formed using the air plasma spray (APS) process. The thicknesses of the top coat were 200 and 400  $\mu\text{m}$ , and those of the bond coat were 100 and 200  $\mu\text{m}$ . TBC samples with a thickness ratio of 2:1 in the top and bond coats were employed in the CFTF and TS tests. After CFTF for 1429 cycles, the interface microstructure of the relatively thick TBC was in a sound condition without any cracking or delamination; however, the relatively thin TBC was delaminated near the interface between the top and bond coats after 721 cycles. In the TS, the TBCs were fully delaminated (> 50%) after 140 and 194 cycles for thicknesses of 200 and 400  $\mu\text{m}$  in the top coat, respectively. These observations allow us to control the thickness of TBC prepared using the APS process, and the thicker TBC is more efficient in improving thermal durability in the cyclic thermal exposure and thermal shock environments.

© 2014 The Authors. Published by Elsevier Ltd. This is an open access article under the CC BY-NC-ND license (<http://creativecommons.org/licenses/by-nc-nd/3.0/>).

Selection and Peer-review under responsibility of the Chairs of The 1st International Joint Mini-Symposium on Advanced Coatings between Indiana University-Purdue University Indianapolis and Changwon National University, Indianapolis.

*Keywords:* Thermal barrier coating; Coating thickness; Air plasma spray; Cyclic thermal exposure; Thermal shock; Thermal durability.

---

\* Corresponding author. Tel.: +82-55-213-3712; fax: +82-55-262-6486.  
E-mail address: [jungyg@changwon.ac.kr](mailto:jungyg@changwon.ac.kr)

## 1. Introduction

Thermal barrier coatings (TBCs) have been applied to the hot components of gas turbines and aeronautical engines, such as turbine blades, vanes, burner transition ducts, and combustor parts, to improve their hot corrosion and oxidation resistances and their service lifetimes [1–3]. The TBC system can provide a major reduction in the surface temperature of the metallic components when combined with the use of internal air cooling. The TBC system can be considered as a four-layered material system, consisting of (1) a substrate of nickel- or cobalt-based superalloy, (2) an oxidation-resistant metallic bond coat of MCrAlY, (3) a thermally grown oxide (TGO) layer, and (4) a ceramic top coating. The oxidation-resistant metallic bond coat (usually MCrAlY powder, where M stands for Co, Ni, or Fe, or a combination of these elements) is typically deposited by means of vacuum plasma spraying, air plasma spraying (APS), low-pressure plasma spraying, or the high-velocity oxy-fuel process. The bond coat provides a rough surface for mechanical bonding of the top coat, protects the underlying substrate against high temperature oxidation and corrosion, and reduces the coefficient of thermal expansions (CTEs) mismatch between the substrate and the top coat [4]. The bond coat surface, onto which the yttria-stabilized zirconia (YSZ) top coat is deposited, has a thin oxide layer that mainly consists of various oxides (NiO, Ni(Cr,Al)<sub>2</sub>O<sub>4</sub>, Cr<sub>2</sub>O<sub>3</sub>, Y<sub>2</sub>O<sub>3</sub>, Al<sub>2</sub>O<sub>3</sub>) [5,6]. The thin TGO layer creates the adhesion (bonding) between the bond and top coats [7]. The insulation top coat of usually 6 to 8 wt% YSZ is deposited either using the APS or electron beam–physical vapor deposition (EB–PVD) process. The top coat has excellent thermal shock resistance and low thermal conductivity, reducing the surface temperature of the cooled components in gas turbine engines at the rate of 4–9 °C per 25 μm [8–10].

In recent decades, the development of advanced coatings and processing methods has been a field of active research in TBCs. Many new techniques, such as solution precursor plasma spraying, electrostatic spray assisted vapour deposition, electron beam-directed vapor deposition (EB–DVD), and EB–PVD have been used to create advanced TBCs [11,12]. The EB–PVD process usually exhibits various superior properties, such as better corrosion resistance, adhesive strength, and surface roughness. However, production of TBCs (which are currently being used in jet aircraft engines to prolong component lifetimes and improve the thrust and efficiency of the engines [13–15]) by the EB–PVD process is complex and expensive. Economical coating methodologies that enable a high degree of control over the coating morphology are desired in land-based gas turbines. The APS process, with its economic benefits, is still preferred commercially, because of the relatively low cost and simple process compared with advanced coating methods such as EB–PVD and EB–DVD. The APS process also has its own advantage in producing the large and complex-shaped TBCs. Numerous factors have to be considered in practical applications of TBCs, such as thermal stability, thermal conductivity, chemical inertness, CTEs, and thermomechanical properties. Among them, the thermal durability in cyclic thermal exposure is an essential factor for the reliability and lifetime performance of the APS–TBC system, which is closely related to its microstructure. In addition, there are many ways to enhance TBC performance, such as controlling the porosity of TBC, employing materials with a low thermal conductivity, and increasing the thickness of TBC [16,17]. The scope of this study was limited to a particular set of APS–TBC samples prepared with different thicknesses in the top and bond coats, as described in Section 3.

In this study, two types of TBC system with different thicknesses in the top and bond coats were prepared using the APS process. The microstructure evolution and thermal durability were investigated through the cyclic furnace thermal fatigue (CFTF) and thermal shock (TS) tests, including the delamination behavior or fracture behavior, to understand the effect of the coating thickness in the APS–TBC system. The relationship between thermal durability and coating thickness of the APS–TBC system is discussed based on the microstructure evolution and hardness variation before and after cyclic thermal exposure.

## 2. Experimental Procedure

### 2.1. Preparation of TBC samples

The nickel-based superalloy GTD-111 was used as the substrate. GTD-111 superalloy has the following nominal composition by weight: Ni = bal. %, Cr = 14.0%, Co = 9.5%, Ti = 4.9%, W = 3.8%, Al = 3.0%, Ta = 2.8%, Mo = 1.5%, C = 0.1%, Zr = 0.03%, and B = 0.01%. The dimensions of the substrate were 25.4 mm diameter and 5 mm

thickness. The substrate was sandblasted using an alumina powder with particle size of 50 mesh, and then the APS processes for the bond and top coats were conducted within 2 h. The bond coat was prepared using AMDRY 962 powder (Sulzer Metco Holding AG, Switzerland, nominal composition of Ni–22Cr–10Al–1.0Y in wt% and particle size of 56–106  $\mu\text{m}$ ). The thicknesses of the bond coat were approximately  $d = 100$  and  $200 \mu\text{m}$ . The top coat was formed on the bond coats using powdered zirconia ( $\text{ZrO}_2$ ) containing 8 wt% yttria (METCO 204 C-NS, hereinafter C-NS; Sulzer Metco Holding AG, particle size of 45–125  $\mu\text{m}$ ). The thicknesses of the top coat were approximately  $d = 200$  and  $400 \mu\text{m}$ . In this study, TBC samples with a thickness ratio of 2:1 in the top and bond coats were prepared. The fabrication parameters for the bond and top coats were as recommended by the manufacturer (Chrome-Alloying Co. Ltd., Hatfield, UK).

## 2.2. Cyclic furnace thermal fatigue and thermal shock tests

A bottom-loading programmable cyclic furnace was used to determine the life cycle of the TBC systems. The CFTF tests were performed for 1429 cycles in the specially designed furnace: one side of the sample was exposed and the other side air-cooled. The surface temperature of the sample was about  $1100 \text{ }^\circ\text{C}$  with a temperature difference of  $150 \text{ }^\circ\text{C}$  between the top and bottom surfaces of the sample with a dwell time of 60 min, followed by natural air cooling for 10 min at room temperature. The failure criterion was defined as 25% buckling or spallation of the top coat in the CFTF. The TBC samples for the TS tests were annealed using a muffle furnace. After reaching  $1100 \text{ }^\circ\text{C}$ , the samples were placed in the furnace. In the TS tests, the samples were held for 60 min in the furnace and then directly quenched in water for 5 min. Throughout the TS tests, the temperature of the water was between 20 and  $35 \text{ }^\circ\text{C}$ . More than 50% of the region spalled in the top coat was adopted as the criterion for failure in water-quenched samples. The TS tests were reported in previous studies while investigating the thermal durability of TBC systems [18–20]. At least five samples were tested for each condition.

## 2.3. Characterization

The selected samples before and after the CFTF and TS tests were preprocessed to observe the cross-sectional microstructure and mechanical properties. The samples were mounted in a fluid epoxy resin, polished using silicon carbide paper and then polished using  $3 \mu\text{m}$  and  $1 \mu\text{m}$  diamond pastes. The cross-sectional microstructures of the TBC samples were observed using a scanning electron microscope (SEM; Model JSM–5610, JEOL, Japan). The thickness of the TGO layer formed at the interface between the bond and top coats after the CFTF and TS tests was measured using the SEM. The hardness values of the bond and top coats before and after the CFTF and TS tests were determined using a microindenter (HM-114, Mitutoyo Corp., Kawasaki, Japan) with a Vickers tip for a load of 3 N [21]. To obtain more reliable values, 10 points were tested for each result. The size of the hardness impression was measured using the SEM and all experiments were performed at room temperature.

## 3. Results and discussion

### 3.1. Microstructure of as-prepared TBCs

The cross-sectional microstructures of as-prepared TBC samples at low magnification are shown in Fig. 1. The microstructures of the TBCs with different thickness configurations of 200/100 and 400/200  $\mu\text{m}$  in the bond and top coats, respectively, are shown in Figs. 1(a) and 1(b). The top and bond coats were well deposited with the designed concept, showing the relatively thin and thick thicknesses. The bond coats of  $116.5 \pm 12.6$  and  $238.1 \pm 16.8 \mu\text{m}$  and the top coats of  $227.0 \pm 14.5$  and  $423.5 \pm 22.4 \mu\text{m}$  in the thin and thick TBC systems, respectively, were well formed by changing the number of coating passes and the spray parameters. The TBC samples were prepared using the APS process. In the APS process, many small particles are accelerated by the high-power plasma to impinge on the bond coat to form the top coat. Therefore, there are intrinsic defects, such as global pores, unmelted particles, splat boundaries, and oxide materials in the top coat. In general, certain amounts of porosity and microcracks are favorable in achieving low thermal conductivity and a high level of thermal shock resistance, because pores and

microcracks accommodate deformation and reduce the stress [22,23]. In addition, the interface microstructures between the top and bond coats of TBCs formed in this study are shown in Fig. 1. The highly magnified interface microstructures of TBCs (Figs. 1(a-2) and 1(b-2)) showed irregular shapes with the formation of a TGO layer less than about  $1\mu\text{m}$  and a sound condition without any global defects, such as cracking and delamination. The bond coat featured a high level of visible oxides.

The interface roughness of the bond coat is one of the most important factors that affects the lifetime of TBC systems [15,24]. However, in another study, it was reported that the APS–TBC lifetime was independent of the average surface roughness [25]. Even though each TBC system in this study showed a slightly different interface microstructure from a microscopic viewpoint, the interface structures were very similar to each other in a macroscopic viewpoint. Oxides in the APS bond coat are generally seen as dark, elongated phases that appear as strings in the microstructure, parallel to the interface. Oxides are produced by particle/atmosphere interaction and/or heating of the coating surface during deposition. Interaction of the hot particles with their surrounding environment, usually air, leads to an oxide film on the particle surfaces. Longer dwell times and higher particle temperatures increase the thickness of the oxide layer on the particles, producing higher concentrations of oxide stringers within the bond coat [26].

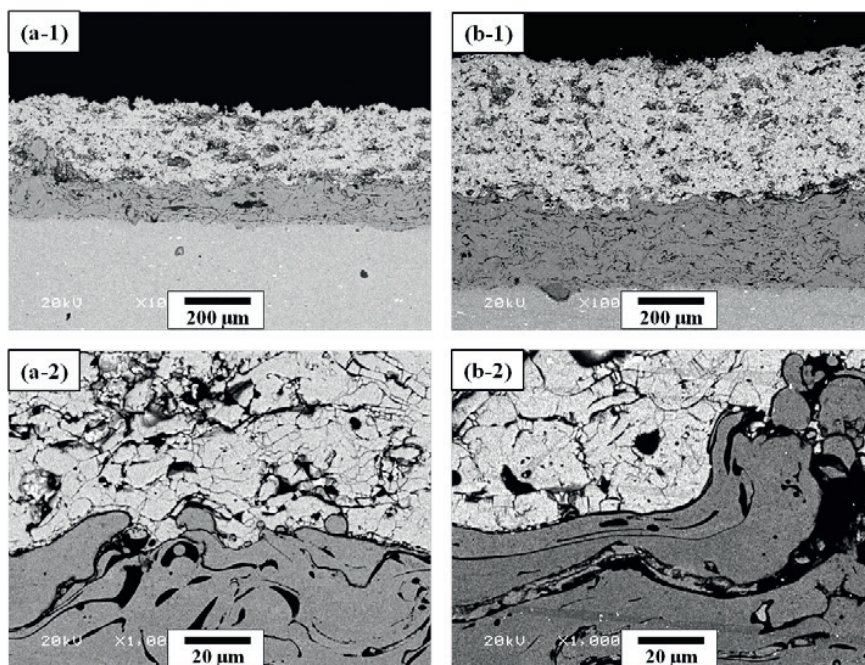


Fig. 1. Cross-sectional microstructures of as-prepared TBCs: (a) TBC with a relatively thin thickness in the top and bond coats and (b) TBC with a relatively thick thickness in the top and bond coats. Each number indicates the overall and interface microstructures, respectively.

### 3.2. Cyclic thermal exposure

The cross-sectional microstructures of TBCs with different thickness configurations in the bond and top coats after the CFTF tests for 1429 cycles are shown in Fig. 2. The thin TBC was delaminated near the interface between the bond and top coats after 690–720 cycles, as shown in Fig. 2(a-1). However, the thick TBC showed a sound condition without delamination after 1429 cycles (Fig. 2(b-1)) and relatively denser microstructures compared with the as-prepared TBC, owing to resintering through cyclic thermal exposure. The nominal thickness of the TGO layer in the thin TBC (Fig. 2(a-2)) was  $2.9 \pm 1.2\mu\text{m}$  after delaminating at 720 cycles, whereas that in the thick TBC (Fig. 2(b-2)) was  $7.3 \pm 1.9\mu\text{m}$  after 1429 cycles. If the thickness of the TGO layer is greater than  $10\mu\text{m}$ , the interface

between the TGO and the top coat normally starts to delaminate and show a failure phenomenon [27,28]. The TGO growth is more related to the bond coat properties and chemistry because  $ZrO_2$  is transparent at high temperature. In this study, the composition of the bond coat was the same in both TBCs. Therefore, it can be concluded that the causes of the difference in the thickness of the TGO layers are the thickness of the top coat and the exposure time. The longer exposure time enhances the thickness of the TGO layer and the “rumpling” at the interface of the top and bond coats. The lifetime of the thick TBCs was about twice that of the thin TBCs. The growth of the TGO layer, the bond coat and the top coat layers causes large residual stresses, which lead to spallation of the TBC [29]. In addition, oxidation of the bond coat leads to a change in sign of stresses because of the smaller CTEs of the TGO layer. It is assumed that small cracks formed in the regions of initial tensile stress at the peak tips before stress conversion and grew into the valleys after stress conversion [30].

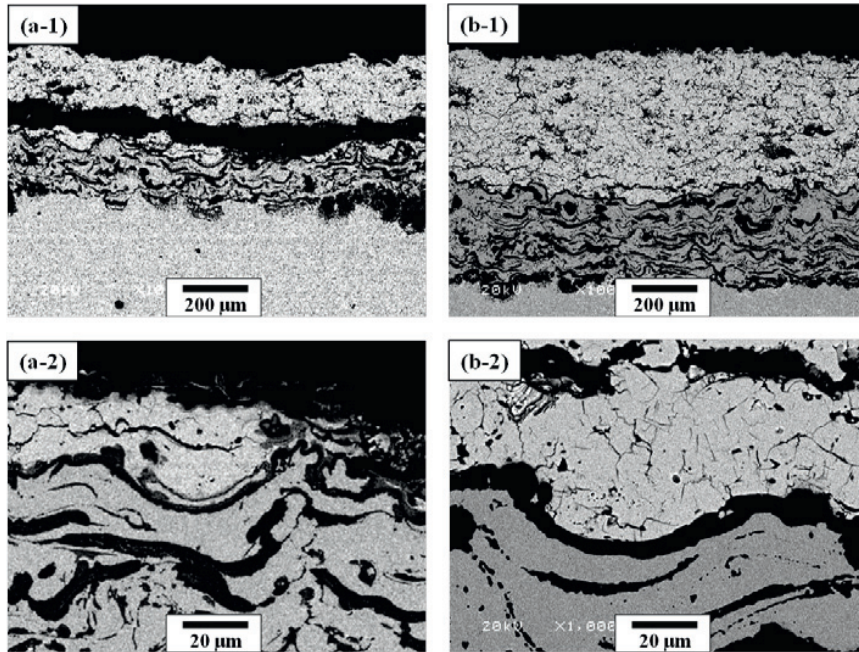


Fig. 2. Cross-sectional microstructures of TBCs after CFTF tests for 1429 cycles: (a) TBC with a relatively thin thickness in the top and bond coats and (b) TBC with a relatively thick thickness in the top and bond coats. Each number indicates the overall and interface microstructures, respectively.

### 3.3. Thermal shock

The TS tests were performed for the two TBC samples with different thicknesses in the top and bond coats. The surface morphologies and cross-sectional microstructures of TBCs after the TS tests are shown in Fig. 3. The thin TBC was delaminated in the range 125–140 cycles, whereas the thick TBC was delaminated in the range 181–194 cycles. In the thick TBC, radial cracks were created from the edge of the specimens because of the relatively higher number of cycles. The cross-sectional microstructures showed a spalling mode after the TS tests in all TBC samples, showing complete delamination near the interface between the TGO and the top coat. The nominal thickness of the TGO layer in the thin TBC (Fig. 3(a-3)) was in the range 6.2–8.1  $\mu\text{m}$  after 140 cycles, whereas that in the thick TBC (Fig. 3(b-3)) was in the range 6.8–8.9  $\mu\text{m}$  after 192 cycles. Normally, the thicker TBC provides a greater temperature drop across the top coat. Thus, the temperature at the interface between the top and bond coats in the thick TBC would be lower than in the thin TBC. In the TS tests, the lifetime of the thick TBC was longer than that of the thin TBC. The result of a previous study is in agreement with our results for the CFTF tests [31]. The result verifies that the thickness in the top coat is one of the important factors for thermal durability of TBC systems,

indicating that the thermal durability of the thick TBC prepared using the APS process was better than that of the thin TBCs. The lifetime of TBCs with different thicknesses after the CFTF and TS tests are summarized in Table 1.

Table 1. The lifetime of TBCs with different thicknesses in the top and bond coats after the CFTF and TS tests.

Test species	Thin TBC (No. of cycles)	Thick TBC (No. of cycles)
Cyclic furnace thermal fatigue (CFTF)	721	1429
Thermal shock test (TS)	125–140	181–194

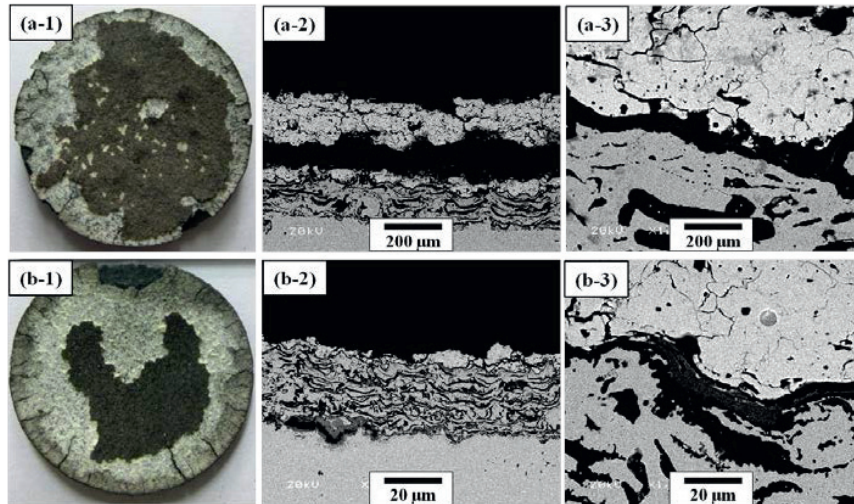


Fig. 3. Surface micrographs and cross-sectional microstructures of TBCs after TS tests: (a) with a relatively thin thickness in the top and bond coats and (b) TBC with a relatively thick thickness in the top and bond coats. Each number indicates surface micrographs, cross-sectional interface microstructures, and highly magnified interface microstructures, respectively.

### 3.4. Hardness

The hardness values of the top coats before and after the CFTF tests are shown in Fig. 4, which were measured using a Vickers indentation method. The indentation tests were conducted on the sectional plane with a load of 3 N at room temperature. The hardness values of the top coats in the as-prepared TBCs were determined to be  $3.3 \pm 0.2$  (mean  $\pm$  standard deviation) and  $3.5 \pm 0.3$  GPa for the thin and thick TBCs, respectively. After the CFTF for 1429 cycles, the hardness value of the top coat was determined to be  $4.1 \pm 0.3$  GPa for the thick TBCs. The slight increase in the hardness values after the CFTF was due to the resintering effect, resulting in a dense microstructure, which is in good agreement with the microstructure evolution shown in Fig. 2(b). After the TS, the top coats in all TBC samples tested were delaminated. Therefore, there was no hardness value for the top coat. The hardness values of the bond coats before and after the CFTF and TS tests are shown in Fig. 5. The hardness values of the bond coats in the as-prepared TBCs were determined to be  $4.1 \pm 0.2$  (mean  $\pm$  standard deviation) and  $4.0 \pm 0.3$  GPa for the thin and thick TBCs, respectively. After the CFTF for 1429 cycles, the hardness values of the bond coats were decreased to  $2.4 \pm 0.2$  and  $3.0 \pm 0.2$  GPa for the thin and thick TBCs, respectively. The hardness values of the bond coats after the TS tests were also decreased to  $2.7 \pm 0.2$  and  $3.2 \pm 0.4$  GPa for the thin and thick TBCs, respectively. In the bond coats, the hardness values were clearly decreased compared with those of as-prepared bond coats, independent of thickness. This result agrees with those of previous investigations [4,30]. Oxidation in the bond coat was similar in both tests. However, the hardness values after the CFTF were slightly lower than those after the TS, which could be explained with the Al deficiency and the volume expansion resulting from the higher number of cycles. Usually, the internal oxidation in the bond coat causes degradation of the mechanical properties [8].

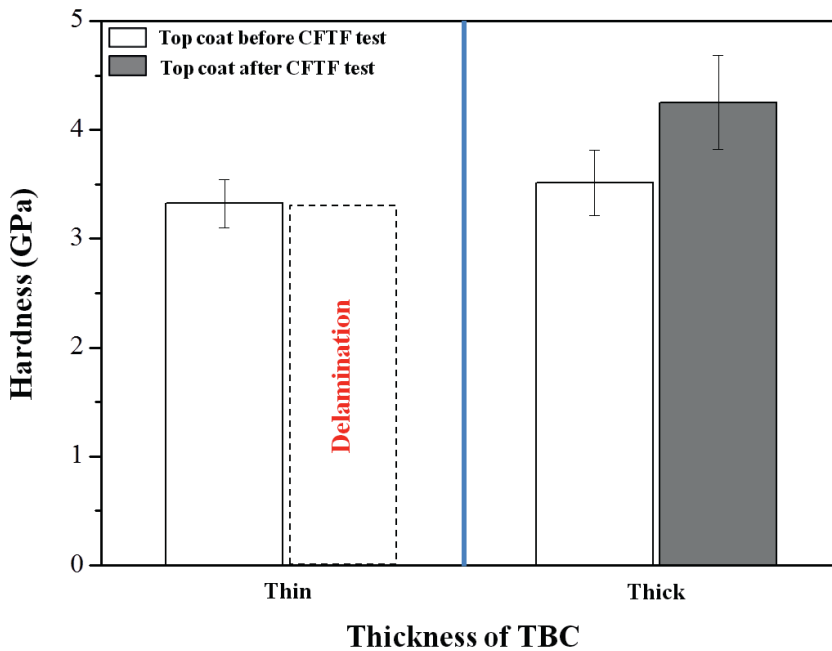


Fig. 4. Hardness values of top coats before and after the CFTF tests. Open and filled marks indicate the hardness values before and after the CFTF tests, respectively.

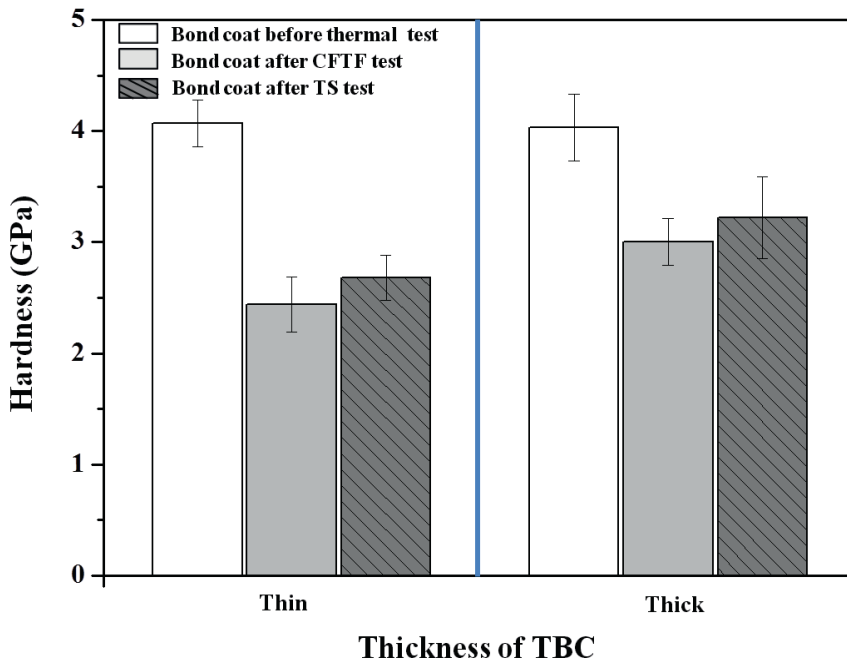


Fig. 5. Hardness values of bond coats before and after the CFTF and TS tests.

#### 4. Conclusions

Two types of TBC with different thicknesses in the top and bond coats have been carefully prepared using the APS process and the effects of thickness configuration on the thermal durability and mechanical properties were investigated and compared systematically through the CFTF and TS tests. The main conclusions in this study can be stated as follows:

1. The TBCs were successfully formed with thicknesses of 200 and 400  $\mu\text{m}$  for the top coat and with 100 and 200  $\mu\text{m}$  for the bond coat. The interface microstructures between the top and bond coats in as-prepared TBCs showed irregular shapes and a sound condition without any cracking or delamination.

2. The CFTF tests showed a sound condition for 1429 cycles for the thick TBC, whereas the thin TBC was delaminated near the interface between the top coat and the TGO after 710–740 cycles. The nominal thickness of the TGO layer in the thick TBC was  $7.3 \pm 1.9 \mu\text{m}$  after the CFTF test for 1429 cycles, while that of TGO layer in the thin TBC was  $2.9 \pm 1.2 \mu\text{m}$  after delaminating at 720 cycles. In the TS test, the thick TBC was delaminated in the range 181–194 cycles, whereas the thin TBC was delaminated in the range 125–140 cycles. These observations verified that the lifetime of the thick TBC was longer than that of the thin TBC. The results obtained in this study are in agreement with those of previous studies.

3. After CFTF tests for 1429 cycles, the hardness value of the top coat in the thick TBC was increased from  $3.5 \pm 0.3$  to  $4.1 \pm 0.3$  GPa. The hardness values of the bond coats after the CFTF tests were decreased from  $4.1 \pm 0.2$  to  $2.4 \pm 0.2$  GPa for the thin TBC and decreased from  $4.0 \pm 0.3$  to  $3.0 \pm 0.2$  GPa for the thick TBC. In addition, the TS tests showed that the hardness values decreased to  $2.7 \pm 0.2$  and  $3.2 \pm 0.4$  GPa for the thin and thick TBCs, respectively.

4. In the TBC system prepared using the APS process, the thick top coat was more efficient in improving thermal durability than the thin top coat in the CFTF and TS environments.

#### Acknowledgements

This work was supported by the National Research Foundation of Korea (NRF) grant funded by the Korean Government (MSIP) (No. 2011-0030058) and the Human Resources Development Program (No. 20134030200220) of the Korea Institute of Energy Technology Evaluation and Planning (KETEP) grant funded by the Korean Government Ministry of Trade, Industry and Energy.

#### References

- [1] X. Zhao, P. Xiao, Mater. Sci. Forum. 606 (2009) 1–26.
- [2] N.P. Padture, M. Gell, E.H. Jordan, Science. 296 (2002) 280–284.
- [3] T.S. Hille, S. Turteltaub, A.S.J. Suiker, Eng. Fract. Mech. 78 (2011) 2139–2152.
- [4] H. Lee, S. Y. Lee, J. Y. Kwon, S. W. Myoung, J. H. Lee, Y. G. Jung, H. Cho, U. Paik, Surf. Coat. Technol. 205(5) (2010) 1250–1255.
- [5] Y. Li, C.J. Li, Q. Zhang, G.J. Yang, C.X. Li, J. Therm. Spray Technol. 19 (1-2) (2010) 168–177.
- [6] Y. Yaslier, S. Alperine, AGARD Report 823, Thermal Barrier Coatings, 1998, pp. 8–10.
- [7] E.Y. Lee, R.D. Sisson, Thermal Spray Industrial Application, Proc. Natl. Therm. Spray Conf, 7th. (1994) 55–59.
- [8] S. W. Myoung, J. H. Kim, W. R. Lee, Y. G. Jung, K. S. Lee, U. Paik, Surf. Coat. Technol. 205 (5) (2010) 1229–1235.
- [9] S.O. Chwa, A. Ohmori, Surf. Coat. Technol. 153 (2002) 304–312.
- [10] I.T. Spitsberg, D.R. Mumm, A.G. Evans, Mater. Sci. Eng. A. 394 (1) (2005) 176–191.
- [11] E.H. Jordan, C. Jiang, J. Roth, M. Gell, J. Therm. Spray Technol. (2014) 1–11.
- [12] P. Song, D. Naumenko, R. Vassen, L. Singheiser, W.J. Quadackers, Surf. Coat. Technol. 221 (2013) 207–213.
- [13] M. Gupta, K. Skogsberg, P. Nylén, J. Therm. Spray Technol. 23(1-2) (2014) 170–181.
- [14] ASTM Standards C633–79. American Society of Testing and Materials: Philadelphia, PA, USA, 1999.
- [15] F. Traeger, M. Ahrens, R. Vaßen, D. Stöver, Mater. Sci. Eng. A. 358 (2003) 255–265.
- [16] X.Q. Cao, R. Vassen, D. Stöver, J. Euro. Ceram. Soc. 24 (2004) 1–10.
- [17] R. Dutton, R. Wheeler, K.S. Ravichandran, K. An, J. Therm. Spray Technol. 9 (2000) 204–209.
- [18] G.M. Ingo, T. Caro, Acta Mater. 56 (2008) 5177–5187.
- [19] P.G. Tsantrizos, G.E. Kim, T.A. Brezinski, Proceedings of AGARD SMP Meeting on Thermal Barrier Coatings, (1997) 71–78.
- [20] R. Knight, X.D. Zhang, E.H. Kim, R.H. Smith, Proceedings of the 15th International Thermal Spray Conference, (1998) 1549–1554.



- [21] X.Q. Ma, M. Takemoto, *Mater. Sci. Eng. A.* 308 (2001) 101–110.
- [22] R. Morrell., *Handbook of Properties of Technical and Engineering Ceramics*, Her Majesty's Stationery Office, London, 1989, pp. 151.
- [23] M. Ahrens, S. Lampenscherf, R. Vaßen, D. Stöver, *J. Therm. Spray Technol.* 13(3) (2004) 432–442.
- [24] B. Rajasekaran, G. Mauer, and R. Vaben, *J. Therm. Spray Technol.* 20(5) (2011) 1209–1216.
- [25] J.R. Davis., *Handbook of Thermal Spray Technology*, ASM International Press, USA, 2004, pp. 48.
- [26] G.C. Chang, W. Pucharoen, *Surf. Coat. Technol.* 32 (1987) 307–325.
- [27] M. Kaka, M.J. Schoenung, *Surf. Coat. Technol.* 205 (2011) 5178– 5185.
- [28] H.J. Jang, D.H. Park, Y.G. Jung, J.C. Jang, S.C. Choi, U. Paik, *Surf. Coat. Technol.* 200 (2006) 4355–4362.
- [29] S. Kuroda, T.W. Clyne, *Thin Solid Films.* 200 (2000) 49–66
- [30] J.A. Haynes, M.K. Ferber, W.D. Porter, *Journal of Thermal Spray Technology.* 9(1) (2010) 38–48.
- [31] T.S. Jang, S.W. Myoung, H.S. Kim, Z. Lu, G.H. Cho, J.H. Lee, Y.G. Jung, *Applied Mechanics and Materials.* 260 (2013) 460–465.